A Mechanistic Study of the Reaction of Iron(III) Porphyrins with Imidazoles. Hydrogen Bonding by the Propionic Acid Side Chains in Hemin Chloride

Meng Qing-jin, Gerard A. Tondreau, John O. Edwards, and Dwight A. Sweigart*
Department of Chemistry, Brown University, Providence, Rhode Island 02912, U.S.A.

A kinetic study is reported for the reaction of [Fe(por)Cl] [por = dianion of protoporphyrin IX (pp) (3,7,12,17-tetramethyl-8,13-divinylporphyrin-2,18-dipropionic acid) or the corresponding dimethyl ester (ppdme)] with imidazole (H-im) or 1-methylimidazole (1Me-im) to give $[Fe(por)(R\text{-}im)_2]Cl$ (R = H or 1-Me). The reaction in acetone goes through a transient green intermediate, [Fe(por)-(R-im)Cl], which was trapped at −78 °C and shown by visible spectroscopic, e.s.r., and conductivity measurements to be high-spin and six-co-ordinate. The reaction is accelerated by hydrogen-bond donors, including H-im, which assist the rate-determining chloride ionization from the intermediate. [Fe(pp)Cl] reacts more than ten times faster than [Fe(ppdme)Cl], and this is shown to be due to enhanced stability of the intermediate and a faster chloride ionization rate with [Fe(pp)Cl]. An explanation is offered that invokes a hydrogen-bonding interaction between an axial ligand and the propionic acid side chains, which were shown not to be deprotonated by imidazole in acetone.

Hydrogen bonding involving the axial ligands in the iron–porphyrin prosthetic group of hemoproteins has received considerable attention. Both 'proximal' and 'distal' type hydrogen bonding have been discussed. Proximal type hydrogen bonding involving an interaction between a co-ordinated (proximal) histidine and a basic site on the polypeptide backbone has been inferred from studies[1–7] of various hemoproteins, and is believed to influence protein structure and reactivity. Evidence for this is also provided by the observation[8] that hydrogen bonding from a co-ordinated imidazole has an effect on the Fe^{III}–Fe^{II} reduction potential in the model compound $[Fe(por)(H\text{-}im)_2]^+$ (por = porphyrin dianion, H-im = imidazole).

Hydrogen bonding of the distal type refers to an interaction between an external (distal) hydrogen donor and an axially co-ordinated ligand such as oxygen. There has been speculation that one function of the E7 distal histidine in hemoglobin (Hb) and myoglobin (Mb) may be to stabilize the polar ion–oxygen bond, usually formulated as Fe^{III}–O_2^-. Recently this has been substantiated by neutron and *X*-ray diffraction studies of Mb–O_2 and Hb–O_2.[9,10] Distal type hydrogen bonding in certain hemoproteins is now established, but the functional significance and energetic role of such hydrogen bonding is not completely clear.

A number of studies of simple metalloporphyrin model systems have appeared that attempt to establish the existence and energetic significance of hydrogen bonding to an axial ligand. We have shown[11] that [Fe(tpp)Cl] (tpp = dianion of 5,10,15,20-tetraphenylporphyrin, see Figure 1) reacts with imidazoles (R-im) to give the transient high-spin six-co-ordinate intermediate [Fe(tpp)(R-im)Cl], which rapidly converts to low-spin $[Fe(tpp)(R\text{-}im)_2]Cl$ according to equation (1). It was found

$$[Fe(tpp)Cl] + 2\ R\text{-}im \longrightarrow [Fe(tpp)(R\text{-}im)_2]Cl \quad (1)$$

that imidazole (H-im) and 1-methylimidazole (1Me-im) give very different rate laws and rate constants. Analysis of these reactions established[12,13] that the rate-determining step in reaction (1) is chloride ionization in the [Fe(tpp)(R-im)Cl] intermediate and that this ionization is accelerated by hydrogen bonding. A similar effect has been found with [Fe(tpp)F] and $[Fe(tpp)N_3]$.[14] Imidazole can serve as the hydrogen donor, as can other species intentionally added to the solution, *e.g.*, H_2O, CF_3CH_2OH, or $CHCl_3$. 1-Methylimidazole cannot hydrogen bond to the departing chloride and this was shown to account for the different rate laws found with H-im and 1Me-im. Even though chloride is not a good Brønsted base, hydrogen bonding by H-im causes a rate acceleration of *ca.* 100. Presumably, more basic axial ligands (F^-, N_3^-, or O_2^-) would be more susceptible to this effect.

Oxygen binding to synthetic iron(II) and cobalt(II) porphyrins is a function of steric, solvation, polarity, and hydrogen-

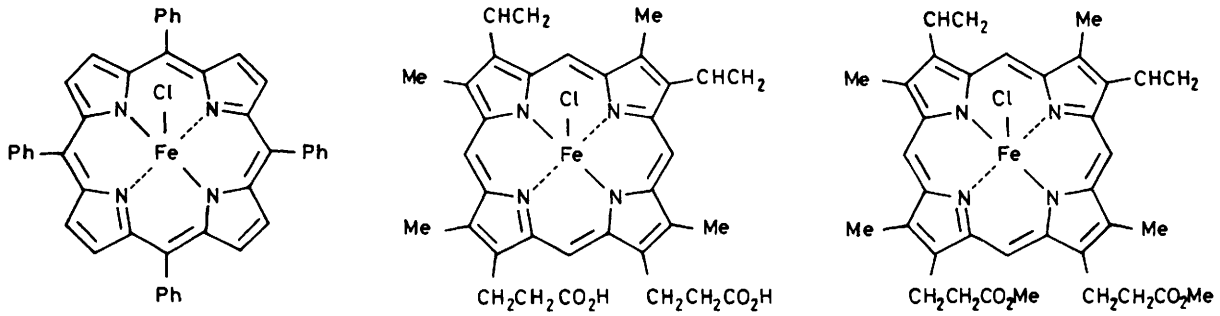

[Fe(tpp)Cl] [Fe(pp)Cl] [Fe(ppdme)Cl]

Figure 1. The iron–porphyrin complexes used in this study

bonding effects.[15-17] Results with 'hanging base' porphyrins suggest that hydrogen bonding to co-ordinated oxygen increases binding by decreasing the O_2 dissociation rate constant.[18] Hydrogen bonding to co-ordinated oxygen affects the rate of oxidation of cobalt(II) porphyrins[19] and increases the oxygen affinity of cobalt(II) Schiff-base macrocycles.[20] Steric and hydrogen-bonding interactions between co-ordinated oxygen or carbon monoxide and distal groups in iron and cobalt 'picket fence' porphyrins have been calculated using *X*-ray data and approximate consistent force field methods.[21] The conclusion is that there is a substantial attraction between O_2 and the amide NH groups even though the N(H) • • • O distance is larger than that normally found in hydrogen-bonded systems. Repulsive contacts with the methyl groups of the pivalamide pocket are also present, though weaker. Both attractive and repulsive interactions were calculated to be less important for the Fe–CO complex. Thus both hydrogen bonding and steric constraints may contribute to reduced CO/O_2 affinity ratios in proteins relative to some model systems.[15,16,21,22] An assessment of distal effects on ligand binding in hemoproteins has been inferred from a comparison of oxygen, carbon monoxide, and alkyl isocyanide binding to the proteins and a chelated protoheme model complex.[22] It was estimated that hydrogen bonding of oxygen to the distal histidine is favoured by 4—8 kJ mol^{-1}.

We now report the results of a mechanistic study of reaction (2), in which por is the dianion of protoporphyrin IX (pp)

$$[Fe(por)Cl] + 2\ R\text{-}im \longrightarrow [Fe(por)(R\text{-}im)_2]Cl \quad (2)$$

(3,7,12,17-tetramethyl-8,13-divinylporphyrin-2,18-dipropionic acid) or the corresponding dimethyl ester (ppdme). As with [Fe(tpp)Cl], reaction (2) involves the formation of reactive high-spin six-co-ordinate intermediates in which hydrogen bonding to the chloride is mechanistically important. However, there are important differences between reactions (1) and (2). Thus, [Fe(pp)Cl] is much more reactive towards H-im than are [Fe(ppdme)Cl] and [Fe(tpp)Cl], which are of similar reactivity. One purpose of this paper is to point out that the propionic acid side chains in [Fe(pp)Cl] apparently are responsible for these reactivity differences.

Pasternack *et al.*[23] previously reported that $[Fe(pp)(dmso)_2]^+$ (dmso = dimethyl sulphoxide) is more reactive than $[Fe(tpp)(dmso)_2]^+$ towards R-im nucleophiles to give $[Fe(por)(R\text{-}im)_2]^+$. These reactions involve a high-spin to low-spin change, and it was proposed that $[Fe(pp)(dmso)_2]^+$ is more reactive because the spin change occurs after the transition state while for $[Fe(tpp)(dmso)_2]^+$ the activated complex is low-spin. We show herein that such an interpretation does not apply to reactions (1) and (2), and that the data may be explained by invoking a hydrogen-bonding role for the propionic acid side chains. We suggest that these side chains in hemoproteins can play a significant role in axial ligand reactivity and that the use of esterified metalloporphyrins to model hemoprotein reactivity may in some cases preclude the observation of an important effect.

Experimental

Solvents were carefully purified as previously described.[12] Imidazole was purified by recrystallization from methylene chloride or by sublimation and 1-methylimidazole was distilled from KOH at reduced pressure. 2,2,2-Trifluoroethanol (Aldrich Gold) was dried over $CaCl_2$, anhydrous 1,10-phenanthroline was dried *in vacuo* for 12 h, and butyric acid was distilled from $KMnO_4$. Hemin chloride, [Fe(pp)Cl], was purchased from Eastman Kodak. $[\{Fe(ppdme)\}_2O]$ was made from hemin chloride by standard methods,[24] and converted to [Fe(ppdme)Cl] by bubbling dry HCl through a methylene chloride solution, and evaporating to dryness.

Table 1. Stability constants (β_2) for reactions (1) and (2) in acetone at 25 °C

Porphyrin	R-im	$10^{-4}\beta_2$/ $dm^6\ mol^{-2}$
tpp	H-im	16
tpp	1Me-im	0.7[a]
ppdme	H-im	7.0
ppdme	1Me-im	1.2
pp	H-im	25
pp	1Me-im	2.2

[a] From ref. 12.

Visible spectra were recorded at room temperature and at −78 °C[13] on Gilford 250 and Perkin-Elmer 552 spectrophotometers. E.s.r. spectra were recorded on a Bruker ER-420 instrument. Conductivity measurements were made with a Beckman RC-16B2 conductivity bridge and a Beckman dipping conductivity cell enclosed in a special apparatus to allow mixing of reactant solutions at any desired temperature.[13] Kinetic experiments at 25 °C were done with a Dionex 110 stopped-flow instrument. Studies at other temperatures were done with a home-made stopped-flow apparatus of the Canterbury design.* This instrument incorporates a Jarrell-Ash Mark X monochromator and Neslab cooling equipment (RTE-8, DCR-4, CC-80), and operates down to −50 °C. All reactant solutions used in kinetic studies were carefully prepared so as to exclude adventitious water. Freshly activated 4 Å molecular sieves were used to dry solvents immediately prior to use, and exposure of reactants and solutions to air was kept to a minimum. Checks were made to ensure that the water-sensitive reaction of the porphyrins with 1Me-im gave reproducible results. Porphyrin solutions were wrapped in aluminium foil to minimize exposure to light. Kinetic runs employed pseudo-first-order conditions, with the porphyrin at *ca.* 10^{-5} mol dm^{-3} and the imidazole nucleophile in at least 100-fold excess.

Optical spectra of transient reaction intermediates were obtained by mixing and recording at low temperatures. They were also recorded by using a Rofin 6000 rapid scanning monochromator mated to a Dionex 110 stopped-flow-instrument. The latter method enables room-temperature spectra to be obtained at a rate of 100 nm ms^{-1}, but gives only moderate resolution. The data from the rapid scanning monochromator were collected by a VK 12-1 transient recorder after triggering the Dionex 110 in the normal manner. A PET 4032 computer was used to collect the data from the transient recorder and to perform the required calculations, which included baseline corrections made by subtracting spectra with and without reactants present. Optical spectra were also obtained from observed absorbance changes recorded during kinetic runs at various wavelengths (see later).

Results and Discussion

Stability Constants.—Table 1 gives the overall stability constants (β_2) for reaction (2) in acetone. These were calculated from static absorbance measurements of [Fe(por)Cl] solutions containing varying concentrations of R-im. Eight data points were obtained for each reaction, with the H-im and 1Me-im concentration in the range 0.0010—0.010 mol dm^{-3} and 0.0030—0.030 mol dm^{-3}, respectively. The data were fitted to

* Designed and built by Dr. N. Rees, University College, Cardiff.

Table 2. Rate constants for reaction (2)

Porphyrin	R-im	Solvent	T/°C	[R-im]/ mol dm^{-3}	$k_{obs.}$/s^{-1}
ppdme	1Me-im	Acetone	25	0.041	0.19
				0.060	0.28
				0.100	0.49
				0.161	0.68
				0.201	0.83
				0.290	1.05
				0.330	1.2
				0.456	1.65
				0.490	1.6
				0.581	1.8
				0.786	2.1
ppdme	1Me-im	Acetone	0	0.0062	0.058
				0.0109	0.066
				0.0252	0.098
				0.0279	0.125
				0.0336	0.13
				0.0497	0.15
				0.0776	0.25
				0.0841	0.255
				0.110	0.31
				0.222	0.47
				0.303	0.53
				0.496	0.60
ppdme	1Me-im	Acetone	−19.8	0.0116	0.021
				0.0232	0.030
				0.0464	0.035
				0.0928	0.047
				0.139	0.057
				0.205	0.061
				0.325	0.062
ppdme	1Me-im	CH_2Cl_2	25	0.0104	2.3
				0.0207	3.2
				0.0363	4.3
				0.0518	5.6
				0.104	9.4
				0.259	18
				0.349	22
				0.581	29
				0.785	35
				0.981	37
ppdme	1Me-im	$CHCl_3$	25	0.0215	11
				0.0286	13
				0.0358	15
				0.0583	20
				0.114	35
				0.286	75
ppdme	H-im	Acetone	25	0.0091	0.40
				0.0227	2.0
				0.0409	7.1
				0.0590	17.5
				0.0816	37
				0.122	78
ppdme	H-im	Acetone	0	0.0013	0.019
				0.009 56	0.17
				0.0319	1.3
				0.0536	5.1
				0.0882	17
				0.107	27
				0.118	33
ppdme	H-im	CH_2Cl_2	25	0.000 92	2.7
				0.001 30	2.9
				0.001 48	3.1
				0.002 35	4.4
				0.003 59	6.4
				0.005 21	8.8
				0.010 4	23
				0.0156	59
ppdme	H-im	$CHCl_3$	25	0.000 54	1.65
				0.001 07	2.3
				0.002 68	5.7
				0.004 29	11
				0.006 44	25
				0.0107	65
pp	1Me-im	Acetone	25	0.0054	3.2
				0.017	4.7
				0.0215	7.75
				0.0272	8.9
				0.0430	12
				0.0700	17
				0.100	20.5
				0.150	24
				0.200	26
				0.300	30
				0.500	29
pp	1Me-im	Acetone	0	0.0034	0.68
				0.0102	2.0
				0.0305	4.2
				0.0474	5.2
				0.0813	6.3
				0.149	6.3
				0.203	6.3
				0.271	6.2
pp	1Me-im	Acetone	−25	0.0034	0.27
				0.0068	0.45
				0.0136	0.82
				0.0272	1.1
				0.0409	1.2
				0.0511	1.2
				0.0681	1.2
				0.0885	1.2
				0.204	1.2
pp	H-im	Acetone	25	0.002 79	3.5
				0.003 56	4.2
				0.004 05	5.1
				0.005 39	7.1
				0.007 74	10.5
				0.0108	18
				0.0151	29
				0.0163	36
				0.0215	54
				0.0251	71
				0.0318	110
pp	H-im	Acetone	−25	0.004 38	2.4
				0.009 48	7.8
				0.0146	13
				0.0190	19
				0.0292	29
				0.0408	41

$$\log(A_0 - A/A - A_\infty) = 2\log[\text{R-im}] + \log\beta_2 \quad (3)$$

equation (3), in which A_0 and A_∞ refer to the absorbances of [Fe(por)Cl] and [Fe(por)(R-im)$_2$]Cl, respectively. Our data, as well as previous work,[25] show that regardless of the R-im concentration, intermediate complexes such as [Fe(por)(R-im)Cl] are not present to a significant extent at equilibrium; in other words the equilibrium constant for the addition of the second R-im is much larger than for the first addition (see later). Equation (3) assumes that the product in reaction (2) is predominantly ion paired (as shown), and this is supported by the fit of the experimental data (correlation coefficient greater than 0.99). Table 1 shows that β_2 is greater with H-im compared to 1Me-im. This has been shown[25] to be due to hydrogen

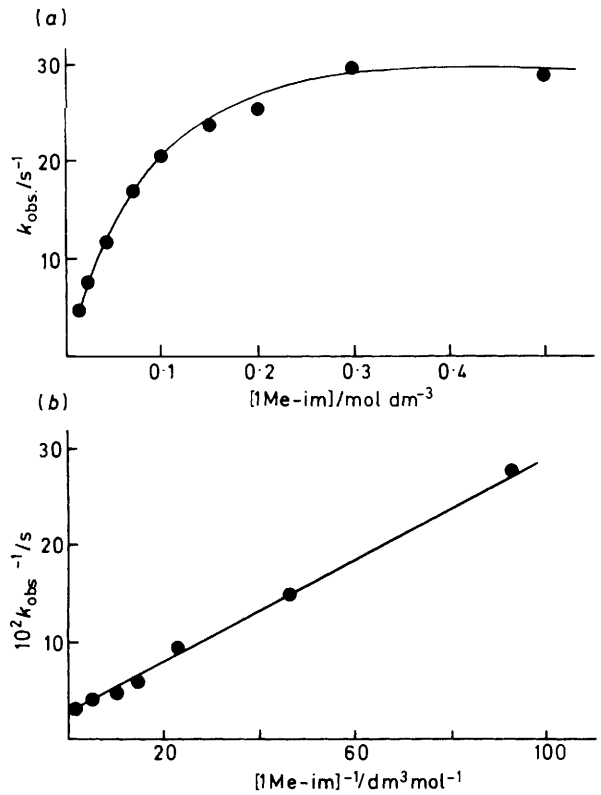

Figure 2. Rate data for [Fe(pp)Cl] + 2 1Me-im ⟶ [Fe(pp)(1Me-im)$_2$]Cl in acetone at 25 °C: (*a*) plot of observed rate constants; (*b*) reciprocal plot of equation (4)

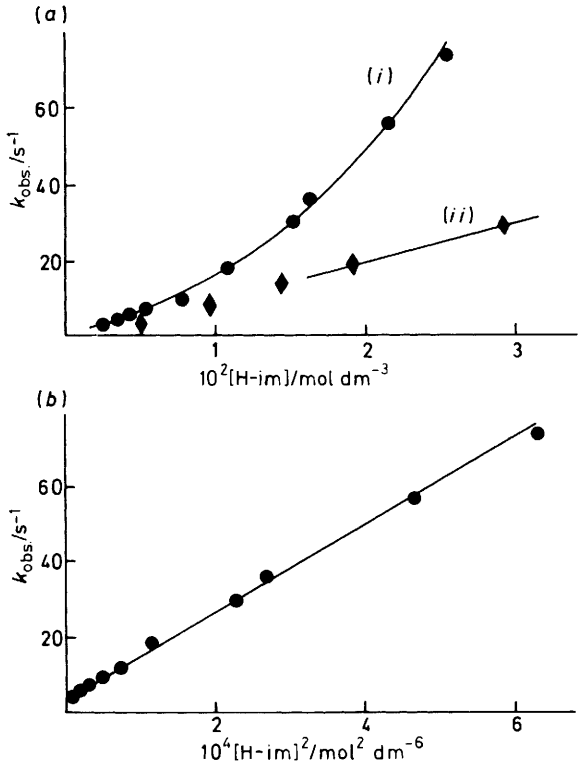

Figure 3. Rate data for [Fe(pp)Cl] + 2 H-im ⟶ [Fe(pp)(H-im)$_2$]Cl in acetone: (*a*) plot of observed rate constants at (*i*) 25 and (*ii*) −25 °C; (*b*) plot of $k_{obs.}$ *versus* [H-im]^2 at 25 °C (the small non-zero intercept is due to the reverse reaction)

bonding of the ionized chloride to co-ordinated H-im in [Fe(por)(H-im)$_2$]Cl. Of course, 1Me-im cannot form such hydrogen bonds.

With [Fe(pp)Cl] as the reactant it is necessary to determine whether or not the R-im nucleophile deprotonates the propionic acid side chains. A potentially simple way to answer this question is *via* conductivity measurements of solutions of [Fe(pp)Cl] and R-im. Deprotonation would generate ionic products. However, such measurements are difficult to interpret because chloride ionization occurs in any case [reaction (2)]. An alternative donor to use is 1,10-phenanthroline (phen) which is a good Brønsted base but does not co-ordinate to the iron or displace chloride from [Fe(por)Cl].[26] We found that the conductivity of [Fe(pp)Cl] in acetone at 25 °C is very low and essentially unaffected by the addition of excess phen. This suggests that phen does not deprotonate [Fe(pp)Cl]. Confirmation of this result was obtained by adding phen and R-im to acetone solutions of butyric acid, which can be taken as a model for the propionic acid groups in [Fe(pp)Cl]. Conductivity measurements in acetone at 25 °C clearly showed that 10^{-3} mol dm^{-3} $CH_3CH_2CH_2CO_2H$ is not deprotonated by 10^{-2} mol dm^{-3} phen or 10^{-2} mol dm^{-3} 1Me-im. Since the pK_a of butyric acid in water is 4.8 while the conjugate acid pK_a's for phen and R-im are 5.0 and *ca.* 7.0, respectively, it is expected that deprotonation of $CH_3CH_2CH_2CO_2H$ and [Fe(pp)Cl] would occur in water. That deprotonation does not occur in acetone is undoubtedly related to the lesser ability of acetone to stabilize the ionic products formed. Previous studies bearing on this issue are inconclusive in that one report[27] states that H-im does not deprotonate the propionic acid groups from [Fe(pp)(H-im)$_2$]$^+$ in dmso whereas another report[28] states that H-im deprotonates [Fe(pp)(CN)$_2$]$^-$ in dmso.

Kinetic Studies.—Most rate measurements of reaction (2) were made in acetone, although other solvents were briefly investigated. Rate data are given in Table 2 and some typical results for [Fe(pp)Cl] are given in Figures 2 and 3. With [Fe(ppdme)Cl] the rate constants ($k_{obs.}$) follow the same functional dependence on the R-im concentration as does [Fe(pp)Cl]. With H-im the rate law is second order in nucleophile, whereas 1Me-im gives a more complicated result (Figure 2). Additionally, it can be seen that H-im is more reactive than is 1Me-im. The Scheme illustrates the mechanism

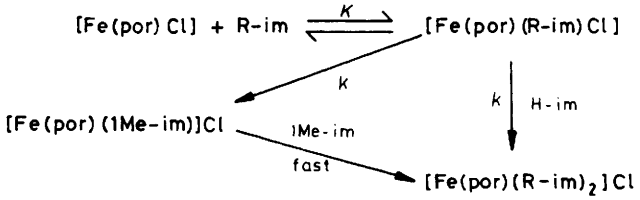

Scheme.

proposed to rationalize the present rate data and that reported previously for reaction (1).[11-13] The first step is the rapid and reversible formation of a six-co-ordinate high-spin intermediate, [Fe(por)(R-im)Cl], which was detected and characterized, as discussed in the next section. With 1Me-im, the rate-determining step is chloride ionization from the intermediate, and this is followed by the rapid addition of 1Me-im to give the low-spin product. With H-im, chloride ionization is also rate determining, but in this case the ionization is assisted *via* hydrogen bonding between the chloride and external H-im. The rate laws required by the proposed mechanism are given by

Table 3. Rate data for reactions (1) and (2) in acetone

Porphyrin	R-im	kK (25 °C)[a]	$\Delta H_{kK}^{\ddagger}$/ kJ mol^{-1}	$\Delta S_{kK}^{\ddagger}$/ J K^{-1} mol^{-1}	k (25 °C)[b]	$\Delta H_{k}^{\ddagger}$/ kJ mol^{-1}	$\Delta S_{k}^{\ddagger}$/ J K^{-1} mol^{-1}	K (25 °C)/ dm^3 mol^{-1}	ΔH_{K}°/ kJ mol^{-1}	ΔS_{K}°/ J K^{-1} mol^{-1}
tpp[c]	1Me-im	14 ± 1.0			3.5 ± 0.4	40.6 ± 2.1	−100 ± 17	3.9 ± 0.3		
ppdme	1Me-im	5.0 ± 0.3	7.9 ± 0.8	−205 ± 33	2.8 ± 0.3	43.9 ± 2.1	−84 ± 8	1.8 ± 0.3	−34.7 ± 2.1	−109 ± 21
pp	1Me-im	390 ± 30	14.6 ± 1.3	−146 ± 21	30 ± 3	38.9 ± 2.1	−88 ± 8	13 ± 1.5	−22.6 ± 2.1	−54 ± 13
tpp[c]	H-im	5 900 ± 300	22.6 ± 0.8	−96 ± 8	450 ± 100			13 ± 3		
ppdme	H-im	5 200 ± 300	22 ± 4	−100 ± 42	580 ± 200			9 ± 3		
pp	H-im	110 000 ± 7 000								

[a] Units are dm^3 mol^{-1} s^{-1} for 1Me-im and dm^6 mol^{-2} s^{-1} for H-im. [b] Units are s^{-1} for 1Me-im and dm^3 mol^{-1} s^{-1} for H-im. [c] Data from refs. 12 and 13.

$$k_{obs.} = \frac{kK[1\text{Me-im}]}{1 + K[1\text{Me-im}]} \quad (4)$$

$$k_{obs.} = \frac{kK[\text{H-im}]^2}{1 + K[\text{H-im}]} \quad (5)$$

equations (4) and (5). These expressions are somewhat simplified in that the chloride ionization step can be written as a reversible one followed by conversion to products. Such a detailed analysis proved useful for reaction (1),[12] but in the present study provides no mechanistic insight beyond that given by equations (4) and (5). Another simplification inherent in equations (4) and (5) is treatment of reaction (2) as irreversible. Except at very low concentrations of R-im, this assumption is a good one. For example, in the reaction of [Fe(pp)Cl] and H-im the effect of reversibility on the rate constants could be detected as a small non-zero intercept (2.5 ± 1.5 s^{-1}) in the plot of $k_{obs.}$ *versus* [R-im]^2 (see Figure 3).

A double reciprocal plot of equation (4) is shown in Figure 2 for [Fe(pp)Cl]. Values of k and K were obtained from the slope and intercept. With [Fe(ppdme)Cl] and 1Me-im, K was also calculated by an independent method based on a comparison of calculated ($A_\infty - A_0$) and observed ($\Delta A_{obs.}$) absorbance changes. In general these two quantities differed in a way that depended on both wavelength and 1Me-im concentration. Equation (6) gives the quantitative relationship assuming the

$$A_\infty - \Delta A_{obs.} = -\frac{1}{K}\frac{A_\infty - A_0 - A_{obs.}}{[1\text{Me-im}]} + A_1 \quad (6)$$

mechanism shown in the Scheme; A_1 is the absorbance of the intermediate. With eight data points over a 1Me-im concentration range of 0.060—0.50 mol dm^{-3}, the fit to equation (6) was excellent, yielding K = 1.6 ± 0.2 dm^3 mol^{-1}. The value of K obtained by the kinetic method (Figure 2) is 1.8 ± 0.3 dm^3 mol^{-1}. Equation (6) was also used to analyse data for [Fe(pp)Cl] and 1Me-im in acetone at −25 °C, with the result that K = 60 ± 20 dm^3 mol^{-1}; the kinetic method gave K = 80 ± 10 dm^3 mol^{-1}.

With H-im as the nucleophile, equation (5) predicts that the rate should become first order in H-im as K[H-im] becomes large. In practice, however, the rate accelerating effect of H-im makes it difficult to use H-im concentrations large enough to demonstrate this at 25 °C. Working at lower temperatures should help, but H-im aggregation then becomes a problem.[13] However, [Fe(pp)Cl] and H-im seem to show the expected saturation effect at −25 °C (Figure 3). Thus a reciprocal plot of equation (5), [H-im]/$k_{obs.}$ *versus* 1/[H-im], for these data gave K = 200 ± 50 dm^3 mol^{-1} and k = 1 200 dm^3 mol^{-1} s^{-1}; the use of equation (6) for this reaction at −18 °C allowed K to be estimated as 100 ± 30 dm^3 mol^{-1}. Similarly, K for [Fe(ppdme)Cl] and H-im at 25 °C was estimated to be 9 ± 3 dm^3 mol^{-1} by using equation (6) over the [H-im] range 0.03—0.10 mol dm^{-3}.

Activation parameters for reaction (2) were obtained in acetone as the solvent. A complete kinetic profile with 1Me-im as the nucleophile was determined at 25 and −25 °C. From these data, activation parameters were calculated for kK, K, and k. The temperature dependence of k was also determined from experiments having the concentration of 1Me-im large enough so that the limiting rate constant k is directly observable as $k_{obs.}$. With [Fe(pp)Cl], k was directly measured at seven temperatures between +25 and −25 °C, and with [Fe(ppdme)Cl] at seven temperatures between +22 and −21 °C. The activation and thermodynamic parameters for k, K, and kK are internally consistent (within error) and are listed in Table 3. With H-im as the nucleophile it was more difficult to measure and interpret the temperature dependence of the rate constants; however, experiments with [Fe(ppdme)Cl] at 25 and 0 °C provided some estimates (Table 3).

The reactions of [Fe(ppdme)Cl] and R-im were studied in CH_2Cl_2 and $CHCl_3$ as well as acetone. With 1Me-im at 25 °C, equation (4) accurately fits the experimental data for all three solvents. The following results were obtained: CH_2Cl_2, k = 40 ± 4 s^{-1}, K = 2.2 ± 0.2 dm^3 mol^{-1}; $CHCl_3$, kK = 250 dm^3 mol^{-1} s^{-1}. For H-im as the nucleophile at 25 °C the results are: CH_2Cl_2, kK = 220 000 ± 20 000 dm^6 mol^{-2} s^{-1}; $CHCl_3$, kK = 530 000 ± 50 000 dm^6 mol^{-2} s^{-1}. The much greater rates in CH_2Cl_2 and $CHCl_3$ compared to acetone are due to the hydrogen-bonding ability of these solvents as measured, for example, by Gutmann acceptor numbers.[29] Thus hydrogen bonding by solvent to the developing chloride ion in the transition state is more important than the solvent dielectric constant, which predicts a rate order opposite to that observed. As far as can be determined, the equilibrium constant K is only weakly dependent on solvent. This argues for little hydrogen-bonding interaction with solvent in the ground state of [Fe(por)Cl] and [Fe(por)(R-im)Cl]. Analogous solvent effects on k and K for reaction (1) have been reported.[12,13]

The addition of the hydrogen bonder 2,2,2-trifluoroethanol (tfe) to the acetone solvent accelerates reaction (2) with 1Me-im. For example, at [tfe] = 0.04 mol dm^{-3}, k increases from 2.8 s^{-1} to 18 s^{-1} for [Fe(ppdme)Cl] and the functional form of the rate law is unchanged. This result shows that hydrogen bonding from tfe is effective at catalysing chloride ionization from [Fe(ppdme)(1Me-im)Cl]. A similar effect is seen with [Fe(pp)Cl], although the increase in k at [tfe] = 0.04 mol dm^{-3} is only a factor of two. 2,2,2-Trifluoroethanol also increases the rate of reaction (2) with H-im, although the rate enhancements are much smaller (≤25% at [tfe] = 0.04 mol dm^{-3}) than seen with 1Me-im. This means that tfe can compete only modestly with H-im for hydrogen bonding in the chloride ionization step.

Characterization of [Fe(por)(R-im)Cl].—The transient inter-

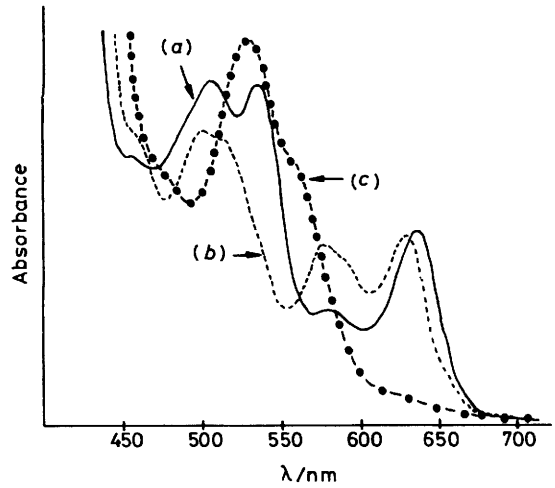

Figure 4. Spectra in acetone at −78 °C of (*a*) [Fe(ppdme)Cl]; (*b*) [Fe(ppdme)Cl] and 1Me-im combined at −78 °C to give [Fe(ppdme)(1Me-im)Cl]; (*c*) solution (*b*) warmed to room temperature and recooled to give [Fe(ppdme)(1Me-im)$_2$]Cl

mediates formed in reactions (1) and (2) participate in the hydrogen-bonding interactions that give rise to the differing behaviour of H-im and 1Me-im as well as the enhanced reactivity of [Fe(pp)Cl] (see later). Accordingly, it is essential that the intermediates be fully characterized. It was noted above that with 1Me-im the use of equation (6) to calculate K from 'time independent' spectral data gave the same value for K as that obtained from use of rate data, equation (4). This proves that formation of the intermediate is indeed responsible for the curvature in $k_{obs.}$ *versus* [1Me-im] plots (Figure 2). Once K is known, equation (6) can be used to calculate A_1 as a function of wavelength, *i.e.*, the optical spectrum of the intermediate can be determined. This was done for [Fe(tpp)(1Me-im)Cl][12,13] and [Fe(ppdme)(1Me-im)Cl] at room temperature. The spectra were also obtained with a Rofin rapid scanning monochromator. Due to the reactivity of the intermediates, room-temperature spectra were of only moderate resolution and were unattainable for the faster reactions, namely ones involving H-im or [Fe(pp)Cl]. However, the use of a low-temperature cell[13] permitted high quality spectra to be obtained at −78 °C, at which temperature some of the intermediates are relatively inert. Figure 4 gives the spectrum of [Fe(ppdme)(1Me-im)Cl], which is similar to that obtained for [Fe(ppdme)(H-im)Cl] and [Fe(pp)(1Me-im)Cl]. Even at −78 °C the latter two species convert within *ca.* 30 min to the final product, [Fe(por)(R-im)$_2$]Cl. Comparison of the results at room and low temperature show that [Fe(por)(R-im)Cl] has virtually the same spectrum regardless of which R-im is present and regardless of the temperature. This shows that H-im and 1Me-im give the same type of intermediate and that the kinetic intermediate is the same as the one trapped at −78 °C. The absorbance maximum at *ca.* 635 nm in the spectrum of [Fe(por)(R-im)Cl] (por = pp or ppdme) shows that these species are high-spin.[30] Interestingly, these complexes are green, in contrast to the reactants or products in reaction (2) which are red or red-brown.

Confirmation of the high-spin nature of [Fe(por)(R-im)Cl] was provided by e.s.r. spectra obtained at −170 °C in acetone. [Fe(ppdme)Cl] gave a typical high-spin spectrum ($g_\perp$ = 6.22). Addition of 1Me-im at low temperature and then quickly freezing gave the green intermediate which has $g_\perp$ = 6.09. Warming the green solution to room temperature and then recooling gave a typical[31,32] spectrum for low-spin [Fe(por)(R-im)$_2$]Cl (g = 2.89, 2.28, 1.55).

The mechanism in the Scheme assumes that [Fe(por)(R-im)Cl] is six-co-ordinate, and that chloride ionization is rate limiting in reaction (2). The kinetic data and activation parameters (Tables 2 and 3, see later) indicate that the intermediate is six-co-ordinate and not a five-co-ordinate ion pair, and that chloride ionization is rate limiting. In order to verify this, conductivity measurements were made at low temperature. At −78 °C in acetone–CH_2Cl_2 (80:20) 10^{-3} mol dm^{-3} [Fe(ppdme)Cl] is non-conducting (Λ_M = 1.1 ohm^{-1} cm^2 mol^{-1}). The addition of excess 1Me-im (10^{-2} mol dm^{-3}) produced the green intermediate, but Λ_M only slightly increased to 2.4. After warming and recooling the solution to give [Fe(ppdme)(1Me-im)$_2$]Cl, the molar conductivity rose to 18. For comparison, 10^{-3} mol dm^{-3} [$PMePh_3$]Br at −78 °C has Λ_M = 30 ohm^{-1} cm^2 mol^{-1}. Similar experiments with H-im or with [Fe(pp)Cl] and R-im showed that the intermediates formed are essentially non-conducting as well, although the conductivity did increase with time as the intermediates slowly reacted with the excess R-im. These results suggest that the intermediate is non-ionic and hence six-co-ordinate.

Mechanistic Role of Hydrogen Bonding.—Before discussing reactions (1) and (2), a few general comments are in order. Hydrogen bonding in transition states is known to be involved in many reactions. An important discovery was the inverse correlation of the ability of solvents to hydrogen bond to anions and the nucleophilic reactivity of the anions. The rates are much higher in dipolar aprotic solvents than in protic solvents due to anion stabilization by the protic solvents.[33] Reactions of substrates other than carbon are influenced by solvent proton-donor ability in a similar manner, *e.g.*, reactions of square-planar platinum(II) complexes have rates dependent on solvent nature.[34] In the reactions of peroxides, hydrogen bonding has been found to be a participant in both transition states and ground states.[35] The interpretation given is that energy-costly charge separation can be avoided if transition states are formed that allow cyclic proton transfer to the leaving anion. A monograph is available dealing with the interactions and consequences of hydrogen bonding in solvent systems.[36]

The discussion of reactions (1) and (2) will deal with various levels of hydrogen-bonding interactions. The simplest case is the reaction of [Fe(tpp)Cl] and [Fe(ppdme)Cl] with 1Me-im, which cannot involve any hydrogen bonding. As Tables 1—3 show, the rate and equilibrium data are very similar, meaning that the electronic effects of substituents on the porphyrin ring are small for these two reactions. The negative values of $\Delta S_k^\ddagger$ are consistent with an ionization process in a solvent of low dielectric constant[37] and the values of ΔH_K° and ΔS° are reasonable for an addition equilibrium. The reaction of [Fe(pp)Cl] and 1Me-im has constants kK, k, and K all greater than for the above two reactions. This seems to be due to a much less negative ΔS_K° (and $\Delta S_{kK}^\ddagger$) and a slightly smaller $\Delta H_k^\ddagger$. A tentative explanation is the breaking of the hydrogen bond between the carboxyl groups and acetone oxygen in order for the carboxyl groups to stabilize an axial ligand (Cl^- or 1Me-im) in the co-ordination sphere. We shall return to this case (see later).

Imidazole reacts with [Fe(tpp)Cl] and [Fe(ppdme)Cl] with comparable rate and equilibrium parameters; again the groups on the porphyrin periphery seem to have little influence. The difference between H-im and 1Me-im is, however, striking, and must be due to the N–H group in imidazole. In dilute solution the N–H would be tied to the acetone oxygen. Upon combination with iron, desolvation by hydrogen-bond cleavage is not required because the imine nitrogen [N(3)] is bonded to the iron. Indeed, because of the acceptor nature of the iron ion, the

N–H · · · $OCMe_2$ bond can be stronger when the imidazole is a ligand. This type of hydrogen bond will in turn stabilize the imidazole–metal link,[26] and should increase the value of K, possibly due to a more negative ΔH°. The available data (Table 3) show the predicted result.

The most obvious difference between the two imidazoles involves the rate laws (second order in H-im but first order in 1Me-im) and the reasons for this (see above). Imidazole assists the chloride ionization by hydrogen bonding. The values of k are larger by more than 10^2 for H-im. The large increase of kK values for H-im over 1Me-im is a consequence of both k and K being enhanced by hydrogen-bond interactions. Since two molecules of H-im are involved in reactions (1) and (2) prior to the transition state, one might expect a more negative $\Delta S_{kK}^{\ddagger}$ for H-im than for 1Me-im. However, this is not the case because one solvent molecule is released from the H-im before it can hydrogen bond to the chloride.

It is relatively easy to pin down the reason why changing from 1Me-im to H-im causes changes in rates and equilibria as seen here for reactions (1) and (2). Assignment of the role of the carboxyl protons is more difficult. We showed above that R-im in acetone does not deprotonate [Fe(pp)Cl]. This means that changing the porphyrin substituents from –COOMe to –COOH is responsible for the large rate enhancements with H-im and 1Me-im (Tables 2 and 3). A simple inductive effect is an unlikely explanation, particularly in view of the lack of substantial substituent effects in the reactions of [Fe(tpp)Cl] and [Fe(ppdma)Cl] (see above). The most obvious interpretation is that the carboxyl proton influences the entry and departure of ligands *via* hydrogen bonding. As mentioned above, the data in Table 3 with 1Me-im show that K is considerably enhanced with pp, and that this is due entirely to a more favourable ΔS_K°. Some of the entropic gain is in fact offset by a *less favourable* ΔH_K°, but the net result is an increase in K. The subsequent chloride ionization step (k) has virtually identical $\Delta S_k^{\ddagger}$ values for all three porphyrins, while $\Delta H_k^{\ddagger}$ is slightly smaller for pp. These results are consistent with a hydrogen-bonding role for the propionic acid side chains. A similar conclusion obtains with H-im as the nucleophile, although in this case fewer rate and equilibrium parameters are available.

Given that hydrogen bonding occurs, the major question to be resolved is which axial ligand in [Fe(pp)(R-im)Cl] interacts with the carboxyl protons. The choices are the chloride or the pyrrole nitrogen in R-im. Models show that the O(H) · · · Cl or O(H) · · · N distance is rather long, but 'doming' or 'ruffling' of the porphyrin core can significantly affect this. Moreover, an interaction of only *ca.* 8 kJ is needed to account for the observed effects, and it has recently been shown [21] that a significant electrostatic hydrogen-bonding interaction occurs even when the electronegative atoms separating the hydrogen are 4 Å apart. Arguments can be made in favour of the hydrogen bonding being to either the chloride or the imidazole pyrrole nitrogen. In either case the formation constant K would be expected to increase, as observed. The increase in the rate constant k for chloride ionization from [Fe(pp)(1Me-im)Cl] is more compatible with hydrogen bonding to the chloride. The results with tfe (see above) also implicate a chloride–carboxyl proton interaction. On the other hand, an imidazole pyrrole nitrogen–carboxyl interaction is suggested by observations that (*a*) changing from tpp to pp or ppdme to pp causes roughly the same rate increase with both 1Me-im and H-im (Table 3), (*b*) ΔH_K° is less exothermic for pp than for ppdme even though K is larger for pp, and (*c*) a rate enhancement with pp occurs when the axial ligand is dmso instead of chloride (see later). Regardless of which axial ligand is involved, the important conclusion is that propionic acid side chains can hydrogen bond to ligands and thereby markedly influence kinetic and thermodynamic behaviour. The interaction is weak free energy-wise, but still more than an order of magnitude in terms of observed rate constants. Furthermore, the interaction seems to be intramolecular and not intermolecular, as indicated by the lack of dependence of $k_{obs.}$ values on porphyrin concentration.

It is interesting to compare the present results with those of Pasternack *et al.*[23] They studied reaction (7), with por = tpp or

$$[Fe(por)(dmso)_2]^+ + 2\ R\text{-im} \longrightarrow [Fe(por)(R\text{-im})_2]^+ + 2\ dmso \quad (7)$$

pp. Both reactions (2) and (7) involve a high-spin to low-spin change, and both give the same product. Nevertheless, the rates and activation parameters would be expected to differ markedly from the present results because the reaction of [Fe(por)Cl] involves an ionization process and a change in co-ordination number of the iron. Indeed, it was found [23] that H-im and 1Me-im react with $[Fe(por)(dmso)_2]^+$ according to the *same* rate law and give similar rates and β_2 values. This verifies our conclusion that the difference between H-im and 1Me-im in reaction (2) is closely tied to the ionization step. Interestingly, Pasternack *et al.*[23] found that $[Fe(pp)(dmso)_2]^+$ is *ca.* ten times more reactive than the tpp complex. Hence the propionic acid groups enhance reactivity even when ionization is not involved. Unlike our results, this rate increase is due to a lowering of $\Delta H^{\ddagger}$ while $\Delta S^{\ddagger}$ is in fact less favourable with pp. However, an interpretation of this result in terms of a possible hydrogen-bonding interaction is difficult because the solvent is dmso and because it is not known if the carboxyl groups are deprotonated by R-im in dmso. The authors offered an explanation in terms of differing locations for the spin change occurring during reaction of the tpp and pp complexes. In support of this, the $\Delta S^{\ddagger}$ values reflected the expected trends for a spin change in an iron(III) porphyrin.[38] It is important to mention, however, that such an explanation based on spin states can definitely be ruled out for reactions (1) and (2). This follows because the [Fe(por)(R-im)Cl] intermediates were shown to be high-spin with subsequent chloride ionization giving nearly identical $\Delta S_k^{\ddagger}$ values regardless of the porphyrin.

Acknowledgements

This work was supported by grants from the National Institutes of Health; D. A. S. is the recipient of a N.I.H. Research Cancer Development Award (1983—1988). M. Q. is grateful to the Peoples' Republic of China and Nanjing University for supporting a two-year leave to visit Brown University. We are grateful to Dr. P. J. Krusic of the DuPont Experimental Station for recording the e.s.r. spectra.

References

1 F. S. Mathews, E. W. Czerwinski, and P. Argos, *Porphyrins*, 1979, **7**, 108.
2 R. Timkovich, *Porphyrins*, 1979, **7**, 241.
3 T. L. Poulos and J. Kraut, *J. Biol. Chem.*, 1980, **255**, 8199.
4 J. Teraoka and T. Kitagawa, *Biochem. Biophys. Res. Commun.*, 1980, **93**, 694; T. G. Spiro, *Isr. J. Chem.*, 1981, **21**, 81; M. Chevion, J. M. Salhany, J. Peisach, C. L. Castillo, and W. E. Blumberg, *ibid.*, 1977, **15**, 311; D. L. Brautigan, B. A. Feinberg, B. M. Hoffman, E. Margoliash, J. Peisach, and W. E. Blumberg, *J. Biol. Chem.*, 1977, **252**, 574.
5 G. N. La Mar and J. S. de Ropp, *J. Am. Chem. Soc.*, 1982, **104**, 5203.
6 G. N. La Mar, J. S. de Ropp, V. P. Chacko, J. D. Satterlee, and J. E. Erman, *Biochim. Biophys. Acta*, 1982, **708**, 317.
7 J. S. Valentine, R. P. Sheridan, L. C. Allen, and P. C. Kahn, *Proc. Natl. Acad. Sci. U.S.A.*, 1979, **76**, 1009.
8 M. M. Doeff, D. A. Sweigart, and P. O'Brien, *Inorg. Chem.*, 1983, **22**, 851; P. O'Brien and D. A. Sweigart, *ibid.*, 1985, **24**, 1405.
9 S. E. V. Phillips and B. P. Schoenborn, *Nature (London)*, 1981, **292**, 81.

10 B. Shaanan, *Nature* (*London*), 1982, **296**, 683.
11 W. W. Fiske and D. A. Sweigart, *Inorg. Chim. Acta*, 1979, **36**, L429; D. A. Sweigart and W. W. Fiske, *NATO Adv. Study Inst. Ser., Ser. C*, 1979, **50**, 315.
12 M. M. Doeff and D. A. Sweigart, *Inorg. Chem.*, 1982, **21**, 3699.
13 G. A. Tondreau and D. A. Sweigart, *Inorg. Chem.*, 1984, **23**, 1060.
14 J. G. Jones, G. A. Tondreau, J. O. Edwards, and D. A. Sweigart, *Inorg. Chem.*, 1985, **24**, 296.
15 G. B. Jameson and J. A. Ibers, *Comments Inorg. Chem.*, 1983, **2**, 97.
16 J. P. Collman, J. I. Brauman, B. L. Iverson, J. L. Sessler, R. M. Morris, and Q. H. Gibson, *J. Am. Chem. Soc.*, 1983, **105**, 3052.
17 K. S. Suslick and M. M. Fox, *J. Am. Chem. Soc.*, 1983, **105**, 3507.
18 M. Momenteau and D. Lavalette, *J. Chem. Soc., Chem. Commun.*, 1982, 341; J. Mispelter, M. Momenteau, D. Lavalette, and J-M. Lhoste, *J. Am. Chem. Soc.*, 1983, **105**, 5165.
19 Z. Dokuzovic, X. Ahmeti, D. Pavlovic, L. Murati, and S. Asperger, *Inorg. Chem.*, 1982, **21**, 1576; D. V. Stynes, H. C. Stynes, J. A. Ibers, and B. R. James, *J. Am. Chem. Soc.*, 1973, **95**, 1142.
20 R. S. Drago, J. P. Cannady, and K. A. Leslie, *J. Am. Chem. Soc.*, 1980, **102**, 6014.
21 G. B. Jameson and R. S. Drago, *J. Am. Chem. Soc.*, 1985, **107**, 3017.
22 M. P. Mims, A. G. Porras, J. S. Olson, R. W. Noble, and J. A. Peterson, *J. Biol. Chem.*, 1983, **258**, 14219.
23 R. F. Pasternack, B. S. Gillies, and J. R. Stahlbush, *J. Am. Chem. Soc.*, 1978, **100**, 2613.
24 J-H. Fuhrhop and K. M. Smith, in 'Porphyrins and Metalloporphyrins,' ed. K. M. Smith, Elsevier Scientific Publishing Co., New York, 1975, ch. 19.
25 F. A. Walker, M. W. Lo, and M. T. Ree, *J. Am. Chem. Soc.*, 1976, **98**, 5552.
26 A. L. Balch, J. J. Watkins, and D. J. Doonan, *Inorg. Chem.*, 1979, **18**, 1228.
27 J-T. Wang, H. J. C. Yeh, and D. F. Johnson, *J. Am. Chem. Soc.*, 1978, **100**, 2400.
28 V. P. Chacko and G. N. La Mar, *J. Am. Chem. Soc.*, 1982, **104**, 7002.
29 V. Gutmann, in 'The Donor-Acceptor Approach to Molecular Interactions,' Plenum Press, New York, 1978.
30 D. W. Smith and R. J. P. Williams, *Struct. Bonding* (*Berlin*), 1970, **7**, 1.
31 J. Subramanian, in 'Porphyrins and Metalloporphyrins,' ed. K. M. Smith, Elsevier Scientific Publishing Co., New York, 1975, ch. 13.
32 M. Momenteau, *Biochim. Biophys. Acta*, 1973, **304**, 814.
33 A. J. Parker, U. Mayer, R. Schmid, and V. Gutmann, *J. Org. Chem.*, 1978, **43**, 1843, and refs. therein.
34 L. Cattalini, V. Ricevuto, A. Orio, and M. L. Tobe, *Inorg. Chem.*, 1968, **7**, 51; R. Romeo, D. Minniti, and S. Lanza, *ibid.*, 1980, **19**, 3663.
35 M. A. P. Dankleff, R. Curci, J. O. Edwards, and H. Y. Pyun, *J. Am. Chem. Soc.*, 1968, **90**, 3209; R. Curci, R. A. DiPrete, J. O. Edwards, and G. Modena, *J. Org. Chem.*, 1970, **35**, 740.
36 'Hydrogen-Bonded Solvent Systems,' eds. A. K. Covington and P. Jones, Taylor and Francis, London, 1968.
37 J. W. Moore and R. G. Pearson, 'Kinetics and Mechanism: A Study of Homogeneous Chemical Reactions,' 3rd edn., John Wiley and Sons, New York, 1981.
38 E. v. Goldammer and H. Zorn, *Biophys. Chem.*, 1975, **3**, 249; H. A. Degani and D. Fiat, *J. Am. Chem. Soc.*, 1971, **93**, 4281.

Received 10*th December* 1984; *Paper* 4/2082